

§ Present address: Department of Physics, University of Texas at Austin, Austin, Tex. 78712.

<sup>1</sup>J. Itoh and Y. Yamagata, *J. Phys. Soc. Japan* **17**, 481 (1962).

<sup>2</sup>F. Simon, *Ann. Physik* **68**, 241 (1922).

<sup>3</sup>H. A. Levy and S. W. Peterson, *Phys. Rev.* **86**, 766 (1952).

<sup>4</sup>J. S. Smart, *Phys. Rev.* **90**, 55 (1953).

<sup>5</sup>O. K. Rice, *J. Chem. Phys.* **22**, 1535 (1954).

<sup>6</sup>C. Domb, *J. Chem. Phys.* **25**, 783 (1956).

<sup>7</sup>C. P. Bean and D. S. Rodbell, *Phys. Rev.* **126**, 104 (1962).

<sup>8</sup>P. C. Mattis and T. D. Schultz, *Phys. Rev.* **129**, 175 (1963).

<sup>9</sup>R. A. Farrel and P. H. E. Meijer, *Physica* **31**, 725 (1965).

<sup>10</sup>C. W. Garland and R. Renard, *J. Chem. Phys.* **44**, 1120 (1966).

<sup>11</sup>M. E. Fisher, *Phys. Rev.* **176**, 257 (1968).

<sup>12</sup>G. A. Baker, Jr. and J. W. Essam, *Phys. Rev. Letters* **24**, 447 (1970).

<sup>13</sup>H. Wagner, *Phys. Rev. Letters* **25**, 31 (1970).

<sup>14</sup>H. Wagner and J. Swift, *Z. Physik* **239**, 182 (1970).

<sup>15</sup>A. J. Wakefield, *Proc. Cambridge Phil. Soc.* **47**, 799 (1951).

<sup>16</sup>C. W. Garland and J. S. Jones, *J. Chem. Phys.* **41**, 1165 (1964).

PHYSICAL REVIEW B

VOLUME 4, NUMBER 3

1 AUGUST 1971

## Order-Disorder Transition in NH<sub>4</sub>Cl. II. Thermal Expansion\*

George E. Fredericks<sup>†</sup>

*Department of Physics and Materials Research Laboratory,  
University of Illinois, Urbana, Illinois 61801*

(Received 3 August 1970)

The thermal expansion of ammonium chloride has been measured in the neighborhood of the order-disorder transition near 242 °K. At 1 atm, the transition is found to be first order with a hysteresis of 0.21 °K. The measured thermal expansion shows sample dependence. The volume-versus-temperature data are fitted using the theory presented in the first paper of this series. These fits show qualitative agreement between theory and experiment, but systematic deviations outside the experimental scatter are found, especially near the transition. Values of the critical exponents  $\alpha_+$  and  $\alpha_-$  of 0.97 and 0.75, respectively, were found to give the best fit to the data, in striking disagreement with theoretical calculations using the Ising Model.

### I. INTRODUCTION

The suggestion that the phase transition of an Ising system on a compressible lattice might become first order has been made by a number of workers.<sup>1-6</sup> Ammonium chloride has been extensively studied in this regard.<sup>7</sup> Since the work reported here was completed, there has been further theoretical work on the compressible Ising system by Baker and Essam,<sup>8</sup> Wagner,<sup>9</sup> and Wagner and Swift.<sup>10</sup> In this later work it is shown that if the lattice spacing is allowed to accommodate locally to the spin fluctuations then the first-order transition of the earlier theory goes away.

However, at 1 atm, the transition in ammonium chloride is first order experimentally. Consequently, a test of these earlier theories for ammonium chloride is still worthwhile. It is quite possible that the results of these earlier theories will find better theoretical justification as time goes on.

One of the most straightforward tests of the theory of the first paper in this series is to see whether or not it can account for the volume-versus-temperature data for ammonium chloride. The thermal expansion of ammonium chloride has been measured by a number of workers. A list of ref-

erences to their work has been compiled by Sakamoto.<sup>11</sup> Boiko<sup>12</sup> has also made a recent measurement of the thermal expansion by x-ray diffraction. We undertook to remeasure the thermal expansion to a higher resolution in order to make a better test of the theory of the transition.

### II. EXPERIMENTAL TECHNIQUE

The temperature of the sample chamber was stabilized by the following method. The chamber was a 1-kg cylinder of copper. This cylinder was suspended in vacuum by two  $\frac{1}{2}$ -in.-diam 0.010-in.-walled stainless-steel tubes. The sample chamber was surrounded by an annular tank filled with liquid nitrogen. A copper flange about 15 cm above the sample chamber provided thermal contact between the nitrogen tank and the stainless-steel tubes. The sample chamber was wound with 70  $\Omega$  of nichrome heater wire. Temperature control then involved supplying the correct power to the heater to balance the heat flow to the nitrogen tank.

A thermistor was glued directly to the heater with thermally conducting epoxy. This thermistor was placed in one arm of a Wheatstone bridge, whose voltage source was the reference output of a PAR JB-5 lock-in amplifier. The off-balance signal of the bridge went to a PAR CR-4 low-noise pream-

plifier and then to the lock-in. The output of the lock-in controlled the heater current by means of a transistor, thus completing the feedback loop. Proper adjustment of the lock-in time constant ensured good proportional control without oscillation. Control to within a millidegree was possible for periods of many days.

The temperature was measured by means of a platinum resistance thermometer, calibrated by the National Bureau of Standards. The thermometer was fixed in a hole near the center of the sample chamber by means of Woods metal. The measurement was made by the standard technique using a Leeds and Northrup K-5 potentiometer and an NBS-calibrated standard resistor. The repeatability of the measurement was  $0.005^\circ\text{K}$  while an independent thermistor showed the sample chamber to be stable to better than  $0.001^\circ\text{K}$ .

The two samples were single crystals about 1 cm in length. They were used to determine the plate spacing of a 5-pF plane parallel-plate capacitor. The capacitance was measured by a General Radio 1615-A three-terminal capacitance bridge. This method of capacitance measurement was suggested to us by Professor Cole.<sup>13</sup> It has the great advantage that all stray capacitances are excluded from the measurement, making possible measurement of 5-pF capacitance to six figures without any drifts due to stray capacitance. The six-figure capacitance accuracy allowed a resolution of  $6 \times 10^{-7}$  in  $\Delta L/L$  given the ratio of capacitor spacing to crystal length that was used.

The design of the framework that translated changes of the crystal's length into changes in capacitor spacing is shown roughly in Fig. 1. The top plate rested on a fused-quartz ring cut from quartz tubing. The quartz ring rested on the same pedestal as the crystal. The crystal was inside the quartz tubing. A hole was drilled in the crystal, and a shaft extended from the bottom of the bottom plate through the crystal and then on through the pedestal on which the crystal sat. A weak spring under the pedestal pulled the bottom plate down onto three steel ball bearings between the bottom of the bottom plate and the top of the crystal.

The thermal contraction of the bottom plate and the steel ball bearings was compensated for by having the crystal sit in a depression in the pedestal. The depth of the depression was calculated such that the spacing between the top and bottom plates would not change with temperature if the crystal were to have no thermal expansion. Consequently any effect due to thermal expansion of the framework could be neglected. Estimates of any residual effect of the framework thermal expansion showed it to be much smaller than the error introduced by edge capacitance.

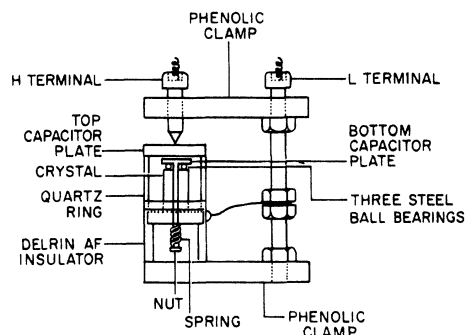


FIG. 1. Sample holder.

Since guard rings were not used, a few words must be said concerning the effect of edge capacitance. An expression for the capacitance of a plane parallel capacitor with square plates is given by

$$C = \frac{\epsilon_0 A}{d} \left( 1 + \frac{2 \ln(\pi a/d)}{\pi a/d} \right), \quad (1)$$

where  $a^2 = A$  is the area of the plates and  $d$  is the plate separation. The second term in Eq. (1) is the contribution of the edge capacitance. The capacitor we used actually had circular plates. Circular plates have a smaller edge-to-surface ratio than square plates. So if we use this square-plate result above to calculate an upper bound on the errors due to edge capacitance, we can be fairly sure that they will not be exceeded for a circular-plate case.

The capacitor that we used had a plate diameter of  $\frac{1}{2}$  in. and a plate separation a little greater than 0.2 mm. These numbers were measured at room temperature. But they still serve to get us into the right range of values for a sample calculation at temperatures near the transition.

We used these numbers to calculate the contribution of the two terms in Eq. (1) to the total capacitance of an equivalent square capacitor. The parallel-plate term contributes roughly 5.5 pF, while the edge term contributes 0.3 pF. So we see that edge capacitance is about 6% of the parallel-plate term.

One might think that the fact that the edge capacitance is so large might make it very difficult to extract any information from capacitance-versus-temperature data. However, this does not turn out to be the case.

The best way to show this is to give the results of a sample calculation. For example, sample 1 exhibited a capacitance range of from about 4.96 to 5.65 pF during the experiment. If Eq. (1) describes the capacitance versus  $d$ , then  $d$  varied roughly from 0.222 to 0.195 mm.

So the sample calculation goes as follows: Equation (1) was used to calculate  $C$  as a function of  $d$

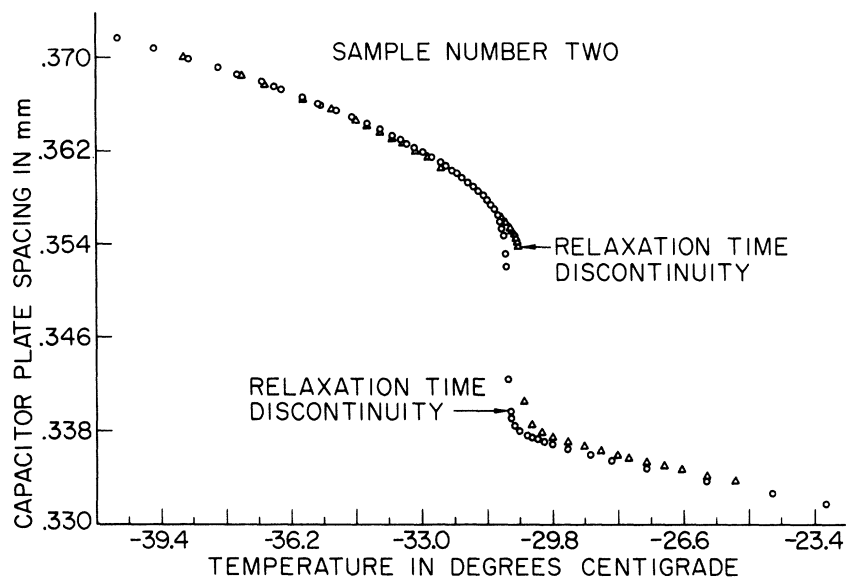


FIG. 2. Raw data for sample 2. Circles were taken with decreasing temperature, triangles with increasing.

over the range  $d=0.225-0.195$  mm. The values of  $C$  thus obtained were used to calculate a number  $d'$  using the relation  $C=\epsilon_0 A/d'$ . So for every  $d$  we started with we have a number  $d'$ .  $d'$  turned out to be about 6% smaller than  $d$ . But the important result comes when  $d'$  is plotted against  $d$ .  $d'$  is, to a very good approximation, a linear function of  $d$ . A straight line was fitted to the  $d'$ -vs- $d$  plot by the least-squares method. When this was done, no  $d'$  value was found to fall further than 0.03% from this straight line.

Consequently, it was assumed that it was safe to ignore the edge capacitance. The values of the plate separation were simply calculated from the relation  $C=\epsilon_0 A/d$ . For this simplification, a price was paid. The price is that the normalization of the experimental  $d$ -vs- $T$  curve such as the one plotted in Fig. 2 is only known to within about 6%. However, it is felt that there would be no systematic error in the shape of the  $d(T)$  curve greater than 0.03% over the whole range.

The true  $L(T)$  is related to our  $d(T)$  by a linear transformation  $L(T)=Ad(T)+B$ . Since the theory we seek to test preserves its form under such a transformation, no attempt was made to do away with the 6% uncertainty mentioned above. However,  $d(T)$  was converted to  $\Delta L(T)/L_0=[d_0-d(T)]/L_0$  before fitting to the theory.  $d_0$  was picked arbitrarily to make  $\Delta L(T)/L_0$  be positive for points above the transition and negative for points below the transition.  $L_0$  was the room-temperature length of the crystal reduced by about 0.5% to reflect the approximate length of the crystal near the transition. Again, it should be stated that the  $\Delta L(T)/L_0$  data presented here are sufficient to test any theory that depends only on the shape of the curve but not

its absolute normalization. The actual tables of data can be obtained from University Microfilms.<sup>14</sup>

After the set point of the temperature controller was changed, the approach to equilibrium could be seen by watching the capacitance value relax to its new value. A few degrees away from the transition, this would take about a  $\frac{1}{2}$  h. Very near the transition it would take many hours. Consequently, an experimental run would usually take about three weeks.

When taking points above but very near the transition on a decreasing temperature run the relaxation time increases slowly as the transition is approached. On continuing to take points on the decreasing temperature run, finally a temperature was reached where a further decrease in temperature of only a fraction of a millidegree would start a relaxation that would not stop for a week or more. The point before this last increment in temperature is the last point used for the fit to the data above the transition. This sudden discontinuity in relaxation time also takes place on an increasing temperature run, except that in this case it takes place at a temperature 0.21 °K higher.

We assumed that these sudden discontinuities in relaxation time are associated with the formation of the ordered phase on the decreasing-temperature runs and the formation of the disordered phase on the increasing-temperature runs. For a quarter of a degree or so after the discontinuity the crystal seems to be a mixture of the two phases.

This is illustrated in Fig. 2. Figure 2 is a plot of some of the points of sample 2. Sample 1 would look similar. The circles are the points of a decreasing temperature run and the triangles are points of the following increasing temperature run.

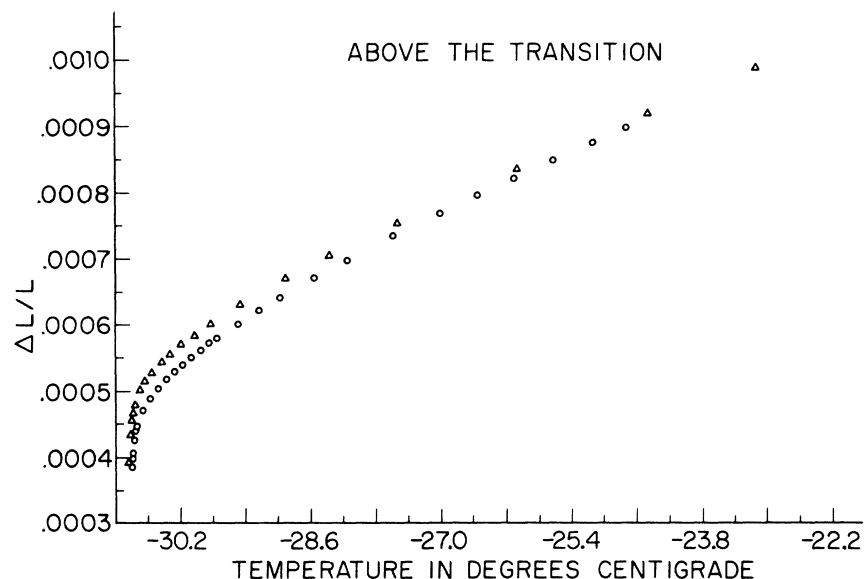


FIG. 3. Comparison of data of samples 1 and 2 above the transition. Circles are sample 1, triangles sample 2.

The points associated with the relaxation-time discontinuities are indicated. It can be seen that the points immediately following the relaxation-time discontinuity in sequence do not have the same volume that they would have if the temperature had been approached from the opposite direction. These points are assumed to represent the coexistence of the two phases and are not used in the fits to the theory.

A further observation should be made with respect to Fig. 2. It is clear from the figure that the capacitor-plate separation is larger after the crystal is cycled through the transition. This is also true of sample 1. A possible explanation for

this is that the crystal becomes plastic and deforms under the slight pressure of the capacitor-plate mounting springs as the crystal goes through the transition. This displacement is allowed for by adding an extra free parameter to the fit.

When the data from the two samples are normalized to each other far from the transition a deviation between the samples becomes apparent. However, the transition still comes at the same place in temperature to within 0.01 °K as defined by the relaxation-time discontinuities. Figures 3 and 4 are above and below the transition, respectively. The circles represent some of the points of sample 1 and the triangles some of the points of sam-

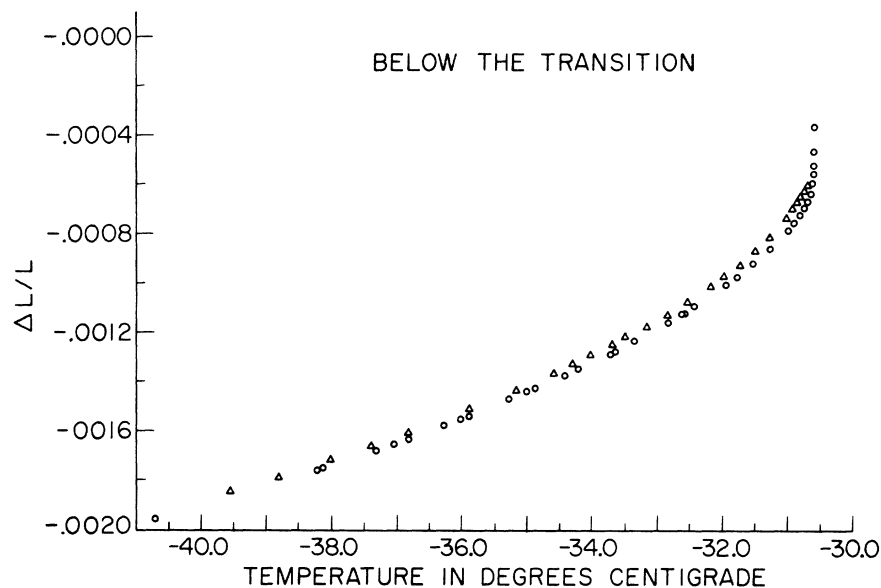


FIG. 4. Comparison of data of samples 1 and 2 below the transition. Circles are sample 1; triangles sample 2.

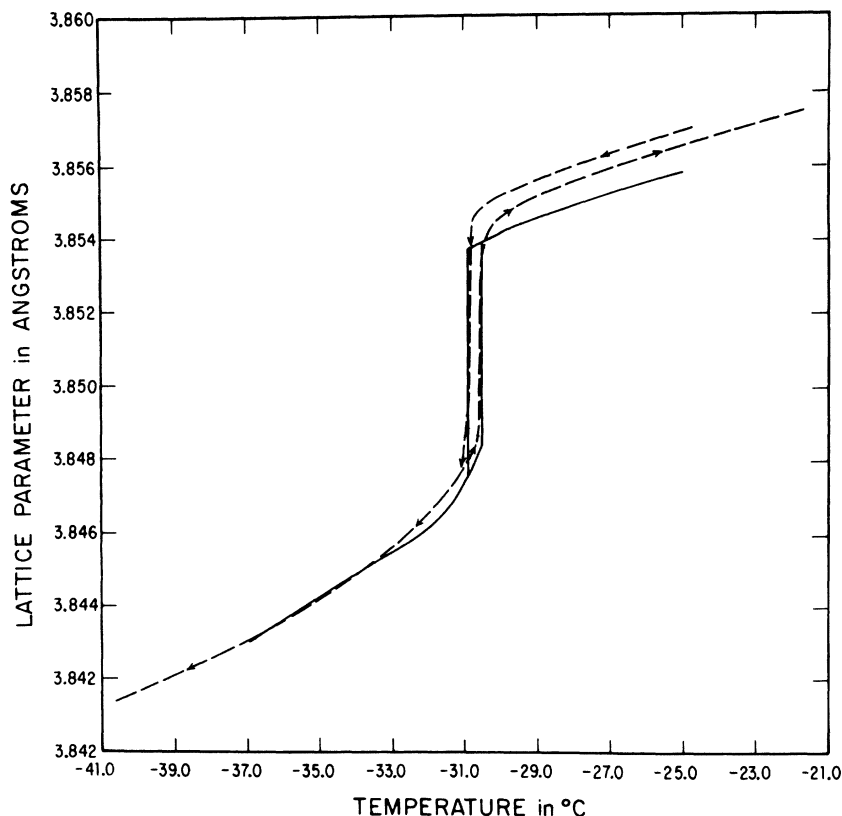


FIG. 5. Comparison to the data of Dinichert. Solid curve is Dinichert's data. Dashed curve is sample 1 normalized to Dinichert's data.

ple 2. The extent of this variation can be seen in the two figures.

### III. COMMENTS ON DATA

The absolute fractional change in length of the crystal from 250 to 232 °K was  $0.30 \pm 0.01\%$  for sample 1 and  $0.31 \pm 0.01\%$  for sample 2. This estimate of error includes the edge capacitance effect. Lawson's<sup>15</sup> data show an all-over variation of 0.50% over this same temperature range. Boiko<sup>12</sup> obtains 0.42% over the same range. Dinichert's<sup>18</sup> data are consistent with the data of Boiko.

The absolute fractional discontinuity in length on going through the transition is much harder to define and compare. First, the  $L(T)$  curve is very steep at the transition. So the size of the apparent discontinuity will depend on how near to the transition the last data point was taken. Second, the next data point taken after going through the transition is characteristic of the coexistence of the two phases. The curve for a quarter of a degree or so after going through the transition is not reproducible. Consequently, the best measure of the jump at the transition is to compare the last point taken above the transition on a decreasing temperature run with the last point taken below the transition on an increasing temperature run. For both samples 1 and 2, there is a discontinuity in the

length of the crystal of 0.08% computed in this way. No such number can be computed for Lawson's or Boiko's data since they show data taken only in one direction. Dinichert shows a discontinuity of 0.14%. Smits, Muller, and Kroger<sup>17</sup> show 0.13% for the discontinuity. The best number of this type for the data of Thomas and Staveley<sup>18</sup> is about 0.1%. This number is difficult to estimate since Thomas and Staveley show equilibrium points on portions of the curve that we experimentally found to be thermodynamically unstable. Their data points are distributed in such a way that there is no way to judge which point is the last point taken above the transition and which point is the last point taken below the transition.

As mentioned above the fractional changes in length from 250 °K reported by various workers disagree. So it is not immediately clear how to compare the shapes of the curves reported by different workers. Figure 5 is an attempt in this direction. Our  $L(T)$  data between -36 and -34 °C were normalized to Dinichert's x-ray diffraction data in the same range. This was done by determining by the method of least squares the linear transformation  $L'(T) = aL(T) + b$  that best brought our data in coincidence with Dinichert's data between these two temperatures. Then this linear transformation was applied to our data over the

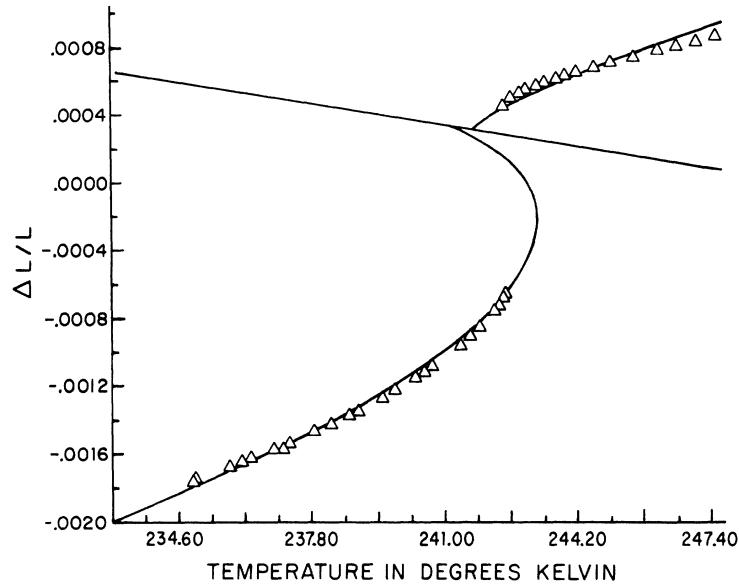


FIG. 6. Best fit to data of sample 1 using Wakefield's series expansion results for  $U_I$ .

whole range of temperature. The result is the dashed curve in Fig. 5. The solid curve is Dinichert's data.

It is interesting to note that when this sort of normalization is made to our data the fractional change in length between 250 and 232 °K shown by our data now becomes greater than that of Dinichert. Also there is an obvious discrepancy in the 3 °K range immediately below the transition.

When a similar normalization is made to Lawson's data, the two curves virtually coincide below the transition. But our over-all fractional change in length from 250 to 232 °K now becomes larger than Lawson's. In addition to this, the slope of our curve comes out noticeably greater than Lawson's above the transition.

So it seems fair to state that the three sets of data, Dinichert's, Lawson's, and the data reported here, are not comparable in detail. However, Boiko's data do compare well with Dinichert's. But Boiko and Dinichert took data by means of x-ray diffraction. The other data were taken by measuring the length of bulk samples. So the difficulty seems to lie with measurements on bulk samples. How these difficulties arise would be interesting to find out.

#### IV. DATA ANALYSIS

Equation (17) of the first paper of this series (preceding paper, this issue) for the case of zero pressure is

$$\frac{\Delta V}{V_0} - \beta_0 (T - T_0) - p_0 \kappa_{T_0} - \kappa_{T_0} \frac{1}{J} \frac{dJ}{dV} U_I \left( \frac{J(V)}{KT} \right) = 0. \quad (2)$$

Equation (22) of the first paper is

$$J = J_0 V_0^n / V^n. \quad (3)$$

Then to a first approximation we have

$$\frac{1}{J} \frac{dJ}{dV} = -\frac{n}{V_0}. \quad (4)$$

Then Eq. (1) can be rewritten

$$\frac{\Delta V}{V_0} - \beta_0 T + (\beta_0 T_0 + P_0 \kappa_{T_0}) + \frac{n \kappa_{T_0}}{V_0} U_I \left( \frac{J(V)}{KT} \right) = 0. \quad (5)$$

This gives  $\Delta V$  as a function of  $T$  implicitly unless an explicit form for  $U_I$  is given. Two different forms for  $U_I$  were tried. The first was the  $U_I$  obtained by Wakefield<sup>19</sup> from the high- and low-temperature expansion of the simple cubic Ising model partition function. In Fig. 6 the curved solid line represents the best fit obtained using Wakefield's  $U_I$ . The straight line is the singular line. The triangles are some of the data points used to obtain the fit. It should be noted that the two segments of the curved line do not join smoothly at the singular line. This is a reflection of the fact that Wakefield's  $U_I$  is not continuous at  $T_c$  for the rigid lattice. This fit overestimates the temperature width of the hysteresis by approximately a factor of 8.

The form for  $U_I$  that produced the best fit was

$$U_I = U_0 \pm U_{\pm} |\epsilon|^{1-\alpha_{\pm}}, \quad (6)$$

where  $\epsilon$  is as given in the first paper:

$$\epsilon = (T - T_0)/T_0 + n \Delta V/V_0. \quad (7)$$

The plus and minus refer to the regions above and below the singular line, respectively.

Using this form for  $U_I$ , Eq. (4) becomes

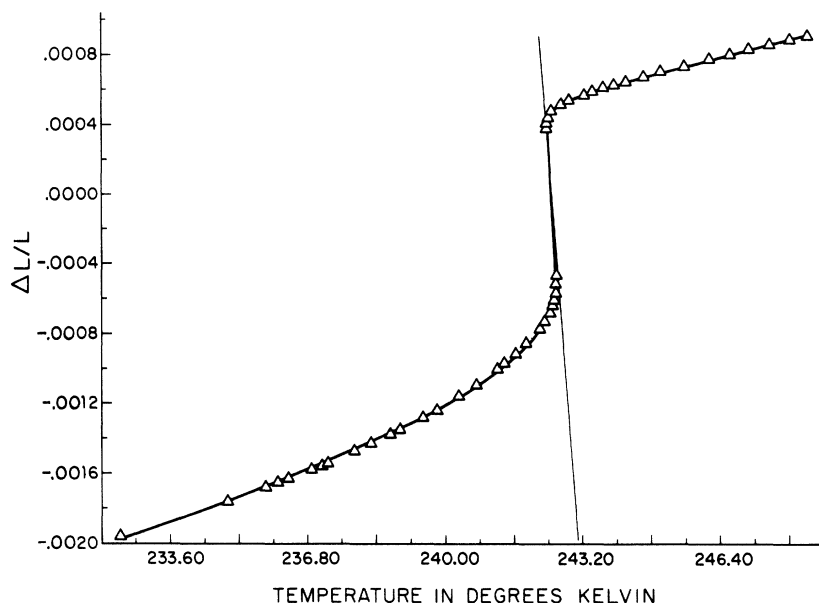


FIG. 7. Calculated curve using parameters of Table I and data points for sample 1.

$$\Delta V/V_0 - \beta_0 T + C_1 \pm C_{\pm} |\epsilon|^{1-\alpha} = 0, \quad (8)$$

where  $C_1$  and  $C_{\pm}$  are just the lumped constants

$$C_1 = (\beta_0 T_0 - P_0 \kappa_{T_0} + U_0), \quad (9)$$

$$C_{\pm} = n \kappa_{T_0} U_{\pm} / V_0. \quad (10)$$

With Eq. (8) there are eight fitting parameters  $\beta_0$ ,  $C_1$ ,  $C_+$ ,  $C_-$ ,  $T_0$ ,  $n$ ,  $\alpha_+$ , and  $\alpha_-$ . This does not count the base-line shift mentioned previously that has to be thrown in to take care of the apparent change in length the crystal suffers on going through the transition. To arrive at a fit to the data the function  $\chi^2$  defined by

$$\chi^2 = \frac{1}{N_A - 6} \sum_{i=1}^{N_A} \left[ \left( \frac{\Delta V}{V_0} \right)_i - \beta_0 T_i + C_1 + C_+ |\epsilon_i|^{1-\alpha_+} \right]^2 + \frac{1}{N_B - 6} \sum_{i=1}^{N_B} \left[ \left( \frac{\Delta V}{V_0} \right)_i - \beta_0 T_i + C_1 - C_- |\epsilon_i|^{1-\alpha_-} \right]^2 \quad (11)$$

was minimized on the computer with respect to the

fitting parameters. The first sum is over the points taken above the transition and the second over the points below the transition.  $N_A$  is the number of points above the transition and  $N_B$  is the number of points below the transition. As mentioned before, the points used above the transition were taken on a decreasing temperature run. The points used below were taken on an increasing temperature run.

It was necessary to fit both sides of the transition simultaneously as shown in Eq. (11). If only one side of the transition were fitted at a time, the best fit would place the singular line in a position with many of the points on the other side of the transition on the wrong side of the singular line. It was found that the best way to force the singular line to pass properly through the hysteresis loop was to fit both sides of the transition simultaneously.

Table I shows the set of parameters that minimize  $\chi^2$  for the data of sample one. Table II is the set that minimizes  $\chi^2$  for sample 2. Figure 7 is a graph of the calculated curve for sample 1 using the parameters of Table I. As many of the data points

TABLE I. Set of fitting parameters for sample 1.

Parameter	Value
$\beta_0$	$1.686 \times 10^{-4}/^\circ\text{K}$
$C_1$	$2.314 \times 10^{-3}$
$C_+$	$2.628 \times 10^{-3}$
$C_-$	$7.974 \times 10^{-3}$
$T_0$	242.48 °K
$n$	0.430
$\alpha_+$	0.967
$\alpha_-$	0.746

TABLE II. Set of fitting parameters for sample 2.

Parameter	Value
$\beta_0$	$1.551 \times 10^{-4}/^\circ\text{K}$
$C_1$	$1.656 \times 10^{-3}$
$C_+$	$1.838 \times 10^{-3}$
$C_-$	$9.779 \times 10^{-3}$
$T_0$	242.55 °K
$n$	0.767
$\alpha_+$	0.963
$\alpha_-$	0.746

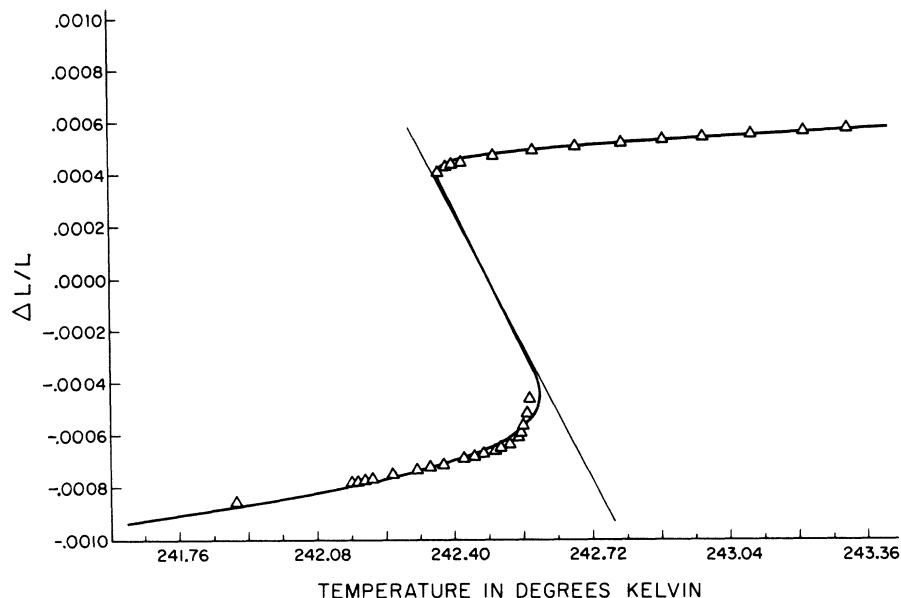


FIG. 8. Expanded scale graph of best fit to sample 1 near the singular line.

are shown as possible. The analogous graph for sample 2 would look similar. Figures 8 and 9 are expanded scale graphs that show the deviation between the data and the fit near the transition for samples 1 and 2, respectively. The diagonal straight lines in Figs. 6-9 are the appropriate singular lines given by the fits. The size of the triangles in the graphs bears no relation to the experimental resolution, which is much greater than the graphs can show.

The function  $\chi^2$  has many other minima. The ones presented here are only the lowest ones that

were found. To make a complete search of the eight-parameter  $\chi^2$  hyperspace would have been prohibitive in computer time. What was actually done was to start with what seemed to be reasonable starting values for the parameters and then let the computer find the nearest minima of  $\chi^2$  automatically.

Attempts were made to find minima closer to the commonly accepted Ising model value of  $\frac{1}{8}$  for  $\alpha$ . This was done by initially constraining  $\alpha$  to be  $\frac{1}{8}$  and finding a minimum of  $\chi^2$  for the remaining parameters. Then the constraint was taken off of

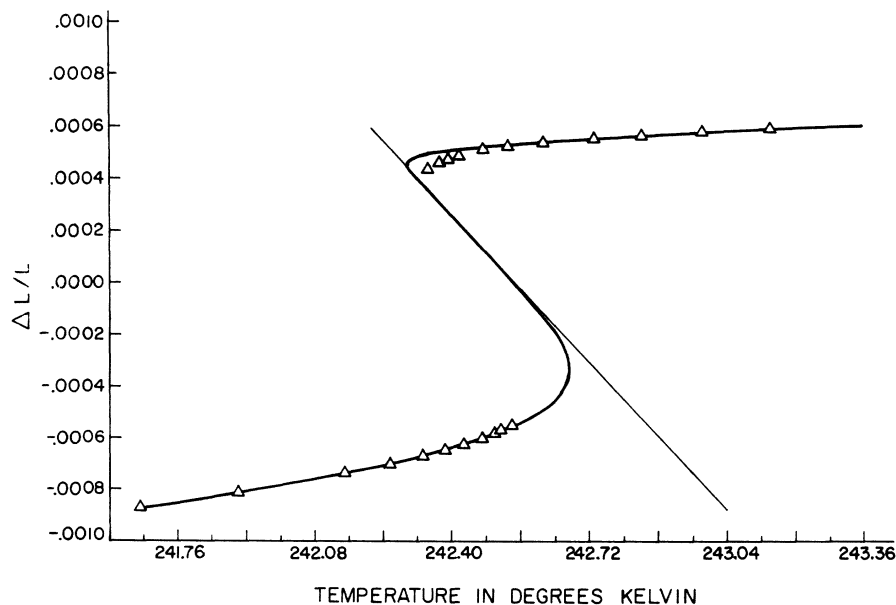


FIG. 9. Expanded scale graph of best fit to sample 2 near the singular line.



TABLE III. Comparison of fitting parameters obtained from the specific-heat and thermal-expansion measurements.

Parameter	Schwartz's work	From Table I	From Table II
$\alpha_+$	0.826	0.967	0.963
$\alpha_-$	0.673	0.746	0.746
$n\beta_0$ ( $^{\circ}\text{K}^{-1}$ )	$4.83 \times 10^{-4}$	$0.725 \times 10^{-4}$	$1.19 \times 10^{-4}$
$a_+/a_-$	0.128	0.400	0.227

$\alpha$  and a minimum in all parameters sought. The minima that were found in this way were orders of magnitude worse than the best ones that are quoted above. Fits were also sought for the case of  $\alpha$  equal to zero. This is the case where the singular term in Eq. (8) is replaced by  $\epsilon \ln(|\epsilon|)$ . The fits found in this case were equally bad.

In the work of Schwartz<sup>20</sup> on the heat capacity of ammonium chloride the same theory of the transition is used to fit the heat-capacity data. Consequently, some of the parameters obtained from the heat-capacity data can be compared to the values of the same parameters obtained from the thermal-expansion measurement. Table III is a list of such parameters. The values of  $a_+/a_-$  in the table are obtained by using the values of  $C_+$  by  $C_-$  in Tables I and II.

## V. CONCLUSIONS

It should be noted that none of the fits shown in the tables are good fits in the  $\chi^2$  sense. In all cases, there is a systematic deviation of the experimental points from the theoretical line. This deviation is much larger than the systematic error arising from edge capacitance. In both this work and the work of Schwartz on the heat capacity, various samples show differences in behavior.

The large  $\alpha$ 's may indicate that first-order nature of the transition actually changes the degree of singularity of the transition. Perhaps the hypothesis of weak coupling goes too far, and local fluctuations in the lattice parameter must be taken into account in calculating the singular terms.<sup>21</sup>

It is unlikely that the number of terms included in the expansion of the lattice free energy and in the expansion of  $\epsilon$  is insufficient since the major deviation between theory and experiment take place near the singular line.

It is possible that sample defects may change the nature of the singular terms in the theory from the forms that were tried in the fitting procedure. For example, in the case of magnetic transitions much better fits can often be found near the transition by assuming that there is a distribution of  $T_c$ 's. We have not attempted to include such effects here. To do so would be rather complicated. It would involve more than introducing a distribution of critical lines. Equation (25) would have to be thought of as true only locally. Then to get the total equilibrium volume Eq. (25) would have to be averaged over the crystal. Since the pressure enters into Eq. (25), this average could not be done until the local strains were known. In any case, this sort of treatment has the effect of making the singularity weaker in the neighborhood of the transition. It seems that in our case what is required for a better fit is a stronger singularity.

But in any case, further attempts to apply theories of this type to ammonium chloride should await a clear understanding of the sample dependence observed in this experiment and that of Schwartz. Ammonium chloride is a very soft and easily damaged material. It would be interesting to study other systems such as MnAs<sup>4</sup> that undergo first-order transitions to see whether the large  $\alpha$ 's found in this experiment and the experiment of Schwartz are also found there.

\* Research supported in part by the U. S. AEC under contract No. AT(11-1)-1198.

† Present address: Department of Physics, University of Texas at Austin, Austin, Tex. 78712.

<sup>1</sup>J. S. Smart, Phys. Rev. **90**, 55 (1953).

<sup>2</sup>O. K. Rice, J. Chem. Phys. **22**, 1535 (1954).

<sup>3</sup>C. Domb, J. Chem. Phys. **25**, 783 (1956).

<sup>4</sup>C. P. Bean and D. S. Rodbell, Phys. Rev. **126**, 104 (1962).

<sup>5</sup>P. C. Mattis and T. D. Shultz, Phys. Rev. **129**, 175 (1963).

<sup>6</sup>R. A. Farrel and P. H. E. Meijer, Physica **31**, 725 (1965).

<sup>7</sup>C. W. Garland and R. Renard, J. Chem. Phys. **44**, 1120 (1966).

<sup>8</sup>G. A. Baker, Jr. and John W. Essam, Phys. Rev. Letters **24**, 447 (1970).

<sup>9</sup>H. Wagner, Phys. Rev. Letters **25**, 31 (1970).

<sup>10</sup>H. Wagner and J. Swift, Z. Physik **239**, 182 (1970).

<sup>11</sup>Y. Sakamoto, J. Sci. Hiroshima Univ. **A18**, 95 (1954).

<sup>12</sup>A. A. Boiko, Kristallografiya **14**, 639 (1969) [Sov. Phys. Cryst. **14**, 539 (1970)].

<sup>13</sup>Robert H. Cole and Paul M. Gross, Jr., Rev. Sci. Instr. **20**, 252 (1949).

<sup>14</sup>G. Fredericks, Ph. D. thesis (University of Illinois, 1969) (unpublished).

<sup>15</sup>A. W. Lawson, Phys. Rev. **57**, 417 (1960).

<sup>16</sup>P. Dinichert, Helv. Phys. Acta **15**, 462 (1943).

<sup>17</sup>A. Smits, G. J. Muller, and F. A. Kroger, Z. Physik Chem. (Leipzig) **B38**, 177 (1937).

<sup>18</sup>D. G. Thomas and L. A. K. Staveley, J. Chem. Soc. **1951**, 1420 (1951).

<sup>19</sup>A. J. Wakefield, Proc. Cambridge Phil. Soc. **47**, 799 (1951).

<sup>20</sup>P. Schwartz, following paper, Phys. Rev. B **4**, 920 (1971), Paper III of this series.

<sup>21</sup>Michael E. Fisher, Phys. Rev. **176**, 257 (1968).